ARTICLE

Direct Observation of Transient Species Generated from Protonation and Deprotonation of the Lowest Triplet of p-Nitrophenylphenol†

Jing Long[a], Zhao Ye[a], Yong Du[b], Xu-ming Zheng[a], Jia-dan Xue[a]*

a. Department of Chemistry, Zhejiang Sci-Tech University, Hangzhou 310018, China
b. Centre for THz Research, China Jiliang University, Hangzhou 310018, China

(Dated: Received on June 22, 2020; Accepted on July 13, 2020)

Photo-induced proton coupled electron transfer (PCET) is essential in the biological, photosynthesis, catalysis and solar energy conversion processes. Recently, p-nitrophenylphenol (HO-Bp-NO_2) has been used as a model compound to study the photo-induced PCET mechanism by using ultrafast spectroscopy. In transient absorption spectra both singlet and triplet states were observed to exhibit PCET behavior upon laser excitation of HO-Bp-NO_2. When we focused on the PCET in the triplet state, a new sharp band attracted us. This band was recorded upon excitation of HO-Bp-NO_2 in aprotic polar solvents, and has not been observed for p-nitrobiphenyl which is without hydroxyl substitution. In order to find out what the new band represents, acidic solutions were used as an additional proton donor considering the acidity of HO-Bp-NO_2. With the help of results in strong ($\sim 10^{-1}$ mol/L) and weak ($\sim 10^{-4}$ mol/L) acidic solutions, the new band is identified as open shell singlet O-Bp-NO_2H, which is generated through protonation of nitro O in ^{3}HO-Bp-NO_2 followed by deprotonation of hydroxyl. Kinetics analysis indicates that the formation of radical $^{\cdot}$O-Bp-NO_2 competes with O-Bp-NO_2H in the way of concerted electron-proton transfer and/or proton followed electron transfers and is responsible for the low yield of O-Bp-NO_2H. The results in the present work will make it clear how the ^{3}HO-Bp-NO_2 deactivates in aprotic polar solvents and provide a solid benchmark for the deeply studying the PCET mechanism in triplets of analogous aromatic nitro compounds.

Key words: Proton coupled electron transfer, Intramolecular charge transfer, Transient absorption, Triplet, nitrophenylphenol

I. INTRODUCTION

Photo-induced proton coupled electron transfer (PCET) has received many attentions [1, 2] in the past decades since it plays an important role in the biological [3–6], photosynthesis [7, 8], catalysis [9, 10], and solar energy conversion [11–13] processes. In general, PCET can take place in three ways: stepwise starting with either electron or proton transfer and concerted electron-proton transfer (EPT) [1]. Understanding the PCET principle allows us to tune and control the reaction process, thereby designing and synthesizing new functional molecules. Recently, p-nitrophenylphenol (HO-Bp-NO_2, Scheme 1) was used as a model compound to study the photo-induced PCET mechanism by using ultrafast spectroscopy [14], which provided a direct evidence for the presence of EPT process. In the system of HO-Bp-NO_2 and amine where intermolecular hydrogen bond would form, two distinct states were observed upon laser excitation, and they were interpreted as conventional intramolecular charge transfer (ICT) state and ICT-EPT photoproduct [14]. The ICT state remains the proton associated with the donor and sequentially transfers the proton to the acceptor. Hammers-Schiffer *et al.* [13, 15] have well explained the configurations [16] of these two states and given a quantitative description on how the population decayed from the ICT state to the EPT state in the singlet manifold by quantum chemistry computation method [17].

In the transient absorption spectra upon laser excitation of HO-Bp-NO_2, not only its singlet but also the triplet exited states exhibit PCET behavior. The substitution of nitro group increases the spin orbital coupling between excited singlet states and the triplet manifold thereby facilitating intersystem crossing [18–20]. The lowest excited triplet state (T_1) can be generated with a great yield [21, 22], so it is also an important PCET pathway that cannot be neglected. When we were exerting a detailed investigation in the triplet manifold starting from the transient absorption experiments on HO-Bp-NO_2 in neat acetonitrile, a new sharp absorption band at 450 nm attracted us since it has not

†Part of the special issue on "the Chinese Chemical Society's 16th National Chemical Dynamics Symposium".
*Author to whom correspondence should be addressed. E-mail: jenniexue@zstu.edu.cn

DOI:10.1063/1674-0068/cjcp2006107

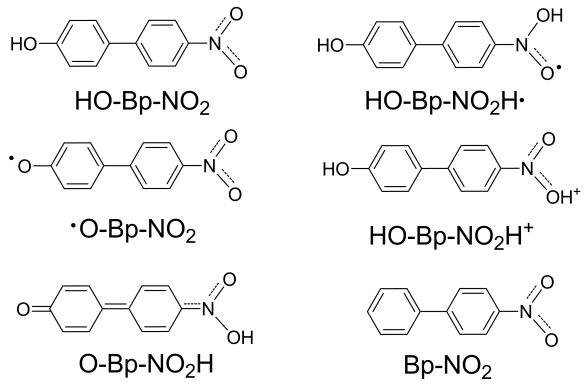

Scheme 1

been observed in analogous nitro aromatic systems [23–27]. What is more, another intermediate/product was also observed to have contribution at 450 nm during the PCET reaction [14]. Thus, finding out the identity of the above new band motivates the present study. After all, understanding all deactivation pathways of T_1 of HO-Bp-NO_2 (^{3}HO-Bp-NO_2) without any other proton acceptors or donors present in the solution is fundamental to investigate its PCET process.

As bearing two functional groups and the torsionable C−C bond connecting two phenyl rings, HO-Bp-NO_2 has some charge separation character [28–30]. On one hand, ICT makes the acidity of HO-Bp-NO_2 increased approximately 9 pK_a units [31] in its excited singlet state, resulting in a strong driving force for proton transfer. On the other hand, the accumulation of electron density on the nitro group makes its basicity enhanced, displaying a strong hydrogen bond accepting ability in the excited triplet state [32]. The coexistence of hydroxyl and nitro groups causes the photochemistry of HO-Bp-NO_2 complicated. Taking its T_1 as an example, as nitro-polycyclic aromatic hydrocarbons (NPAHs) have been revealed that their triplets are able to abstract hydrogen atom from aromatic phenol proceeding by PCET, HO-Bp-NO_2 was expected to undergo a similar reaction and to produce two radicals HO-Bp-NO_2H$^{\cdot}$ and $^{\cdot}$O-Bp-NO_2 (structures are shown in Scheme 1). Proton transfer reaction from the ground state HO-Bp-NO_2 to ^{3}HO-Bp-NO_2 was also possible if considering the proton donating ability of hydroxyl group in HO-Bp-NO_2. Intermolecular proton transfer from hydroxyl to nitro group within two ^{3}HO-Bp-NO_2 molecules were also proposed. Therefore, in the present study acidic solutions were used to provide an additional proton donor so as to help identify what the 450 nm sharp band represents. With the evidences obtained in strong and weak acidic solutions, the new band was recognized as a transient species generated from protonation of nitro O in ^{3}HO-Bp-NO_2 followed by deprotonation of hydroxyl. In order to make the assignment readable, transient absorption spectroscopic results in acidic solutions are presented firstly, and then those in neat acetonitrile are shown. Kinetic results are used to acquire the relationship of the observed species and figure out their reaction pathways. Time-dependent density functional theory (TDDFT) calculations were performed to predict vertical transition energies of candidate species and to help to assign the experimental observation bands. We hope the results in the present work can make it clear how the ^{3}HO-Bp-NO_2 deactivates in aprotic polar solvents such as acetonitrile, dichloroethane and so on, and provide a solid benchmark for the deeply studying the PCET mechanism in triplets of analogous aromatic nitro compounds which is also our future work.

II. EXPERIMENTS AND CALCULATIONS

p-Nitrophenylphenol (98%), p-nitrobiphenyl (98%), 1-naphthol (99%), perchloric acid (72%, AR) were purchased from J&K scientific without further purification. Spectroscopic grade of acetonitrile, cyclohexane, 2-propanol, and methanol were used to prepare sample solutions.

The nanosecond transient absorption (ns-TA) measurements were performed on a LP-920 Laser flash photolysis setup (Edinburgh Instruments, UK). The 355 nm pump laser pulse (pulse width 10 ns and pulse energy 80 mJ) was obtained from the third harmonic output of an Nd:YAG Q-switched laser, and the probe light was provided by a 450 W Xe arc lamp. These two light beams were focused onto a 10 mm quartz cell. The kinetic and spectral signals analyzed by a symmetrical Czerny-Turner monochromator were detected by a photomultiplier (Hamamatsu R928) combined with oscilloscope and an ICCD (Andor, Oxford Instruments) respectively. All solutions used in ns-TA experiments were purged with argon so as to remove oxygen.

Vertical excitation energies and oscillator strengths were obtained using time-dependent density functional theory (TDDFT) [33–35] after the geometry optimization and vibrational frequency computation using (U)B3LYP/6-311++G(d,p) [36, 37] level of theory. All of the quantum mechanical calculations were done using Gaussian software [38].

III. RESULTS AND DISCUSSION

A. ICT character in S_1 and T_1

The ground state (S_0) p-nitrophenylphenol (HO-Bp-NO_2) has the maximum absorption at 338 nm in acetonitrile, red-shifts compared with that (319 nm) in cyclohexane, corresponding to the $S_0 \rightarrow S_1$ transition from HOMO to LUMO localized on phenol and nitrobenzene respectively based on the theoretical calculation (FIG. S1 in supplementary materials). The lowest excited singlet state (S_1) has the absorption maximum at 440 nm [14], similar to the radical cation of phenol (PhOH$^{\cdot+}$)

DOI:10.1063/1674-0068/cjcp2006107

[39]. This suggests the ICT character in S_1. As for a "pure" ICT state, its absorption spectrum should correspond to the sum of spectrum of components, anion radical and cation radical [40]. The ICT imparts the hydroxyl of HO-Bp-NO_2 an enhanced hydrogen bond donating ability, so that in 2-propanol and methanol the absorption maximum shifts to 345 nm and 340 nm respectively. Excitation of HO-Bp-NO_2 with 355 nm laser pulse produces its lowest excited triplet state (T_1) through an ultrafast intersystem crossing [14]. The T_1 of HO-Bp-NO_2 (^{3}HO-Bp-NO_2) has the absorption maximum at 650 nm in acetonitrile (FIG. 1), some red-shifts compared to that in dichloroethane (630 nm) [14] and in cyclohexane (530 nm, FIG. S2 in supplementary materials). The possibility of a charge transfer complex of T_1 with the solvent can be excluded, as the red shift is not in the direction of decreasing ionization potential of the solvent (9.88 eV, 11.07 eV, and 12.20 eV for cyclohexane, dichloroethane and acetonitrile respectively). The observed shift of the absorption maximum corresponding to the $T_1 \rightarrow T_n$ transition in solvents with dielectric constants D_1 and D_2 can be determined by Eq.(1) and Eq.(2) [41].

$$\Delta E_{1-2} = \Delta\mu_{T_1 \rightarrow T_n} \cdot \frac{\mu_{T_1}}{a_3} \Delta_{1-2} f(D) \quad (1)$$

$$\Delta_{1-2} f(D) = \frac{2(D_1 - 1)}{(2D_1 + 1)} - \frac{2(D_2 - 1)}{(2D_2 + 1)} \quad (2)$$

ΔE_{1-2} is the shift of absorption maximum expressed in energy. μ_{T_1} is the dipole moment of T_1 state and a is the cavity radius of the molecule. Here the contribution from the difference of refractive indices of the solvents was negligible. Hence, the T_n state should have a larger dipole moment than T_1. The dipole$_{solvent}$↔dipole$_{T_n}$ interactions reduce the energy of T_n to a larger extent than that of T_1, resulting in the red shift of $T_1 \rightarrow T_n$ transition in the polar solvents. This result indicates that HO-Bp-NO_2 has certain ICT character in the triplet state.

B. Protonation of T_1 in strong acidic solution

The ICT character makes the nitro O in HO-Bp-NO_2 protonated more easily in T_1 than in S_0 [32]. S_0 of HO-Bp-NO_2 still keeps its neutral form in acetonitrile solution with 0.38 mol/L $HClO_4$ (*viz.* strong acidic solution thereafter), this is due to that the UV-Vis absorption spectrum is identical to that in neat acetonitrile. Yet the TA spectrum looks quite different from the neutral T_1 as shown in FIG. 1. In strong acidic solution, two absorption bands with maxima at 445 and 650 nm show almost the same decay time constant of ~650 ns under argon condition. The lifetime of these two bands is sensitive to O_2 and ferrocene. As a result they are identified to T_1 of the protonated HO-Bp-NO_2. TDDFT calculations were performed on the triplet cation ^{3}HO-Bp-NO_2H^+ (proton bonded to nitro O, Scheme 1) to predict its vertical transitions. The results show 692, 453 and 440 nm with oscillator strength f=0.1054, 0.2630, and 0.3829 respectively. This agrees very well with the experimental observation as displayed in FIG. 1. Meanwhile the triplet cation cannot be $^3H_2{}^+$O-Bp-NO_2 (proton bonded to hydroxyl O) for two reasons: firstly, the electron density on hydroxyl group is less in T_1 than in S_0 due to ICT, so it is much harder to be protonated in T_1 than in S_0; secondly, vertical transitions of $^3H_2{}^+$O-Bp-NO_2 predicted by TDDFT calculation are 375 nm (f=0.2098) and 533 nm (f=0.1031). This is not consistent with the experimental spectral observation. Thus the transient species generated in the strong acidic solution is ^{3}HO-Bp-NO_2H^+ (see Scheme 1 for its structure).

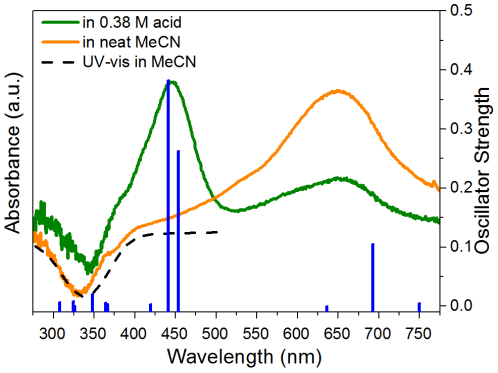

FIG. 1 The transient absorption spectra obtained immediately after the laser excitation of HO-Bp-NO_2 in acetonitrile (MeCN) solution without acid (orange) and with 0.38 mol/mL $HClO_4$ (green). Blue bars represent vertical transitions of ^{3}HO-Bp-NO_2H^+ predicted by TDDFT calculation. A scaled UV-Vis spectrum of HO-Bp-NO_2 in MeCN (dashed line) is also provided for comparison.

C. Protonation and deprotonation of T_1 in weak acidic solution

FIG. 2 and FIG. S4 (supplementary materials) display TA spectra in acetonitrile solution with the 10^{-4}–10^{-3} mol/L acid present (*viz.* weak acidic solution thereafter). At the beginning time delayed in FIG. 2, the neutral triplet ^{3}HO-Bp-NO_2 can still be observed. It should be noted that when ^{3}HO-Bp-NO_2 decays a sharp band rather than a broad absorption arises at 450 nm. To assign the 450 nm sharp band, p-nitrobiphenyl (Bp-NO_2, Scheme 1) was examined for comparison. In FIG. 3, in solutions with the acid 0.01 mmol/L–0.12 mol/L, the appearance of TA spectra changes gradually. For example, in weak acidic solutions the neutral triplet (^{3}Bp-NO_2) is dominant (λ_{max}=514 and 555 nm). When the concentration of acid increasing, ^{3}Bp-NO_2 is less and the triplet cation (^{3}Bp-NO_2H^+) becomes more (λ_{max}=507 nm). Here ^{3}Bp-NO_2H^+ was identified based on the similar reasons

DOI:10.1063/1674-0068/cjcp2006107

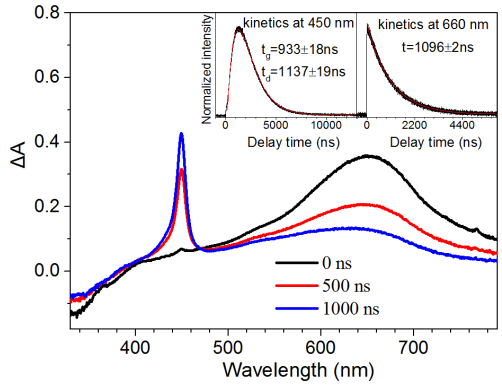

FIG. 2 Nanosecond transient absorption spectra upon laser excitation of HO-Bp-NO_2 in acetonitrile in the presence of 0.1 mmol/L acid. Insert: (black) kinetics monitored at 660 and 450 nm, and (red) exponential curves fitted with a single decay (660 nm) and a combined (growth and decay) functions respectively.

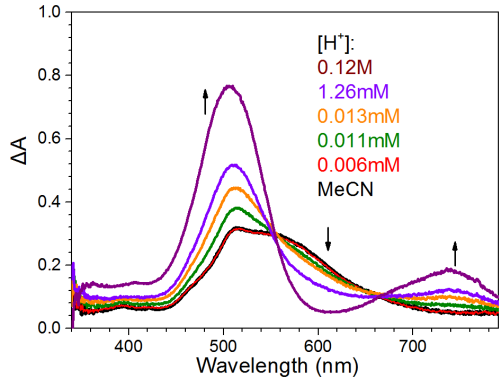

FIG. 3 Nanosecond transient absorption spectra obtained immediately after laser excitation of Bp-NO_2 in acetonitrile solution containing various concentrations of $HClO_4$.

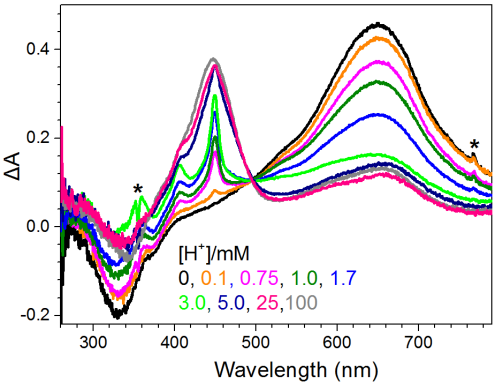

FIG. 4 Nanosecond transient absorption spectra obtained immediately after laser excitation of HO-Bp-NO_2 in acetonitrile solution containing various concentrations of acid. Symbol star indicates the residual of excitation laser pulse.

to that of ^{3}HO-Bp-NO_2H^+. Thus all spectra recorded in acidic solutions can be attributed to the sum of ^{3}Bp-NO_2 and ^{3}Bp-NO_2H^+ in different proportions. But it is not the case for HO-Bp-NO_2 as mentioned above. It is only in weak acidic solutions that the 450 nm sharp band appears. In addition, the band is absent for Bp-NO_2. Hence it could result from the deprotonation of hydroxyl in ^{3}HO-Bp-NO_2H^+. O-Bp-NO_2H (Scheme 1) was explored in its triplet and singlet configurations with DFT calculations. The results show that the open-shell singlet is the lowest in energy. It is 1.4−3.8 kcal/mol lower than the close-shell singlet depending on the functional and the basis set used. Moreover, the calculation predicts the vertical transition at 501 nm with f=1.2606 for the open-shell singlet. This agrees better with the experimental observation than the triplet one that has major vertical transitions at 475, 363, and 342 nm with f=0.0816, 0.2234, and 0.1184. Thus the 450 nm sharp band in weak acidic solutions was assigned to the open-shell singlet O-Bp-NO_2H (O-Bp-NO_2H hereafter). The molecular structure and the spin density contribution of O-Bp-NO_2H are provided in FIG. S3 in supplementary materials. Table S1 in supplementary materials represents its full vertical transitions and corresponding oscillator strengths. This assignment is consistent with the ICT character in ^{3}HO-Bp-NO_2. As the ICT induces the hydroxyl of ^{3}HO-Bp-NO_2 to be able to transfer proton to amine [14], it is reasonable that its acidity would be enhanced in ^{3}HO-Bp-NO_2H^+. However it is seldom seen that sharp peak is in electronic absorption spectra. FIG. S4 in supplementary materials presents TA spectra of HO-Bp-NO_2 in acetonitrile with different concentrations acid, where the 450 nm sharp band was reproducible.

In weak acidic solutions, the decay at 660 nm (^{3}HO-Bp-NO_2) obeys a single exponential function. The kinetics curve at 450 nm has a quasi-symmetrical shape no matter how fast it rises. Fitting the kinetics data at 450 nm with a double exponential function is shown as the inserted in FIG. 2 and FIG. S5 (supplementary materials), and the time constants are presented in Table I. The decay at 450 nm is always a little slower than its growth, and correlates with the decay at 660 nm. Thus the 450 nm sharp band should come from ^{3}HO-Bp-NO_2 since the fast step in a consecutive reaction corresponds to the growth in kinetics. And the protonation of nitro group is slower than the succeeding deprotonation of hydroxyl (reaction (2) in Scheme 2), resulting in that ^{3}HO-Bp-NO_2H^+ is unobservable in weak acidic solutions. By plotting of the pseudo-first decay rate constants at 660 nm against the concentration of acid, the second order reaction rate constant of ^{3}HO-Bp-NO_2 with acid was obtained k_1=(8.3±0.9)×10^9 $(mol/L)^{-1}s^{-1}$. The growth kinetics at 450 nm viz. the decay of O-Bp-NO_2H is also dependent on the concentration of acid, and the rate constant is k_3=(7.8±0.3)×10^9 $(mol/L)^{-1}s^{-1}$. These results further support the mechanism of the consecutive reaction with the reverse kinetics (Scheme 2). The forward rate constant of pathway (2) is faster than

DOI:10.1063/1674-0068/cjcp2006107

TABLE I Pseudo first order decay or/and growth time constants fitted with exponential functions at wavelengths of 660 and 450 nm obtained upon excitation of HO-Bp-NO_2 in acetonitrile containing various concentration of acid.

$[H^+]$/(mmol/L)	d_{660}[a]/ns	d_{450}[b]/ns	g_{450}[c]/ns
0.05	1845	1907	1590
0.1	1095	1137	889
0.2	623	662	442
0.3	431	422	351

[a] Decay at 660 nm,
[b] Decay at 450 nm,
[c] Growth at 450 nm.

$$^3\text{HO-Bp-NO}_2 \underset{-H^+}{\overset{+H^+}{\rightleftharpoons}} {}^3\text{HO-Bp-NO}_2\text{H}^+ \underset{+H^+}{\overset{-H^+}{\rightleftharpoons}} \text{O-Bp-NO}_2\text{H} \quad \begin{matrix}(1)\\(2)\end{matrix}$$

Scheme 2

that of pathway (1), thus resulting in the decay kinetics of O-Bp-NO_2H should be also dependent on the concentration of acid, and display the similar second order reaction rate constant with that of ^{3}HO-Bp-NO_2 and acid (8.3×10^9 $(\text{mol/L})^{-1}\text{s}^{-1}$) [42].

The proton bonded to nitro O in ^{3}HO-Bp-NO_2H^+ has an acidity constant value of pK_a=3.1 which is estimated according to results from its homologs. Both ^{3}Bp-NO_2 (FIG. S6) and T_1 of 4-amino-4′-nitrobiphenyl [32] have similar values of pK_a=3.1. In TA spectra recorded in weak acidic solutions (10^{-4}−10^{-3} mol/L) in FIG. 4, ^{3}HO-Bp-NO_2 and O-Bp-NO_2H were major species with little ^{3}HO-Bp-NO_2H^+. Thus the hydroxyl in ^{3}HO-Bp-NO_2H^+ was estimated to have an acid dissociation constant of pK_a=2.6.

D. Intermolecular proton transfer from S_0 to T_1

As mentioned in the introduction section, a small but distinct band at 450 nm was observed upon excitation of HO-Bp-NO_2 in neat acetonitrile as shown in FIG. 5(a). After removal of the absorption of ^{3}HO-Bp-NO_2 at 650 nm, the 450 nm band shape can be presented clearly (FIG. 5(b)). According to the reults obtained in strong and weak acidic solutions, the 450 nm band was recognized as O-Bp-NO_2H. It may originate from the reaction of T_1 with S_0 rather than T_1 with T_1. Table II and FIG. S7 (supplementary materials) display that the formation of O-Bp-NO_2H (decay component at 450 nm) is correlative with the decay of ^{3}HO-Bp-NO_2 (decay at 650 nm). Both of them are dependent on the concentration of ground state HO-Bp-NO_2. The equilibrium constant (K) of the reaction of T_1 with S_0 (reaction (3) in Scheme 3) is only pK_a=7.6 since the acidity of HO-Bp-NO_2 pK_a=10.7 (FIG. S8). But the reaction moves forward due to the large K in reaction (4) so that O-Bp-NO_2H is able to be produced with an observable yield.

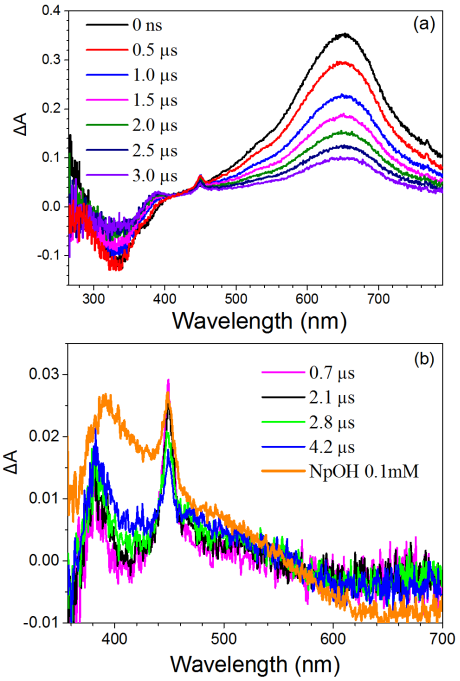

FIG. 5 (a) Nanosecond transient absorption spectra recorded at various time delays after laser pulse excitation of HO-Bp-NO_2 (0.05 mmol/L) in neat acetonitrile. (b) Difference spectra obtained by subtraction of scaled 0 ns spectra from those recorded at post time delays which have been labeled in the graph, with the criterion of completely removing the absorption of ^{3}HO-Bp-NO_2 at 650 nm, and 1.0 μs spectrum (orange) in solution in the presence of 0.1 mmol/L NpOH.

E. Competetion reaction in neat acetonitrile

The transient absorption intensity of O-Bp-NO_2H is much smaller in neat acetonitrile (FIG. 5(a)) than in weak acidic solutions (FIG. 2). If assuming proton transfer is the major decay pathway of T_1, based on parameters in Table III the relative yield of O-Bp-NO_2H over ^{3}HO-Bp-NO_2 is 73% (the concentration of HO-Bp-NO_2 0.05 mmol/L) while this value is 86% in weak acidic solutions (the concentration of acid 0.1 mmol/L). This result indicates that there must be some decay pathways to compete with the formation of O-Bp-NO_2H in neat acetonitrile. Fortunately, an intermediate in this way was caught by transient absorption spectra as shown in FIG. 5(b). The formation time constant in 380 nm correlates with the decay of ^{3}HO-Bp-NO_2 (Table II). The intermediate with a characteristic band at 380 nm was assigned to the radical $^{\cdot}$O-Bp-NO_2, this was based on the analogous radical in references [39] and its vertical transitions (391 nm, f=0.4503) predicted by DFT calculation.

There could be two channels (reaction (5), and reac-

TABLE II Pseudo first order decay or/and growth time constants fitted with exponential functions at wavelengths of 650, 450 and 380 nm obtained in neat acetonitrile with different concentration of HO-Bp-NO_2 (in mol/L).

[HO-Bp-NO_2]	d_{650}[a]/ns	g_{450}[b]/ns	d_{450}[c]/ns	g_{380}[d]/ns
3.2×10^{-5}	3417	978	3437	3078
4.9×10^{-5}	2553	853	2509	2500
5.6×10^{-5}	2295	772	2220	2023

[a] Decay at 660 nm;
[b] Growth at 450 nm;
[c] Decay at 450 nm;
[d] Growth at 380 nm;

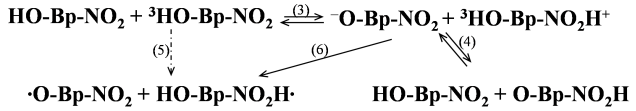

Scheme 3

tions (3)+(6) in Scheme 3) to compete with the generation of O-Bp-NO_2H and to form radical ·O-Bp-NO_2. Reaction (5), one hydrogen atom abstraction, can proceed in four ways: hydrogen atom transfer, electron followed proton transfer, proton followed electron transfer and concerted electron-proton transfer (EPT). The hydrogen atom transfer was excluded since the observed second order reaction rate ($\sim10^9$ $(\mathrm{mol/L})^{-1}\mathrm{s}^{-1}$) is too fast to take place in this way [43]. However, we cannot exclude that reaction (5) could proceed in a EPT mechanism with the rate close to diffusion. In the hydrogen bonded ^{3}HO-Bp-NO_2+HO-Bp-NO_2 complex (formed during reaction (3)), the reduction and the oxidation potentials of the hydrogen acceptor and donor can be decreased [44]. It is more likely for reaction (6) to take place because hydrogen bonded complex can decrease Gibbs free energy of electron transfer. What is more, the electron transfer is easier to undergo from an anion to a cation. Thus reactions (5) and/or (6) may compete with reaction (4) and are responsible for the low yield of O-Bp-NO_2H in neat acetonitrile.

IV. CONCLUSION

Nanosecond TA spectra upon 355 nm laser excitation of HO-Bp-NO_2 in neat acetonitrile measured a sharp band at 450 nm accompanying with the decay of ^{3}HO-Bp-NO_2 at 650 nm. These two absorption bands have correlative kinetics dependent on the concentration of HO-Bp-NO_2. In order to identify the 450 nm sharp band, various concentrations of acid were used to provide an extra proton donor. In strong acidic solution ($\sim10^{-1}$ mol/L), the transient species carrying two major broad bands at 445 and 650 nm was recognized as ^{3}HO-Bp-NO_2H$^+$ according to the ICT character of ^{3}HO-Bp-NO_2 and TDDFT predictions. In weak acidic solutions (10^{-4}−10^{-3} mol/L), a sharp band at 450 nm was obtained during the decay of ^{3}HO-Bp-NO_2. This 450 nm sharp band is similar to the observation in neat acetonitrile. By comparison with transient absorption spectra of Bp-NO_2 which is without hydroxyl substitution, the 450 sharp band nm was assigned to an open-shell O-Bp-NO_2H species based on DFT calculations. Thus, in ^{3}HO-Bp-NO_2H$^+$ the proton of hydroxyl is more acidic than the one bonded to nitro group. In neat acetonitrile, there is a parallel way originated from the reaction of ^{3}HO-Bp-NO_2 and HO-Bp-NO_2 to compete with the formation of O-Bp-NO_2H. This way could occur through concerted electron-proton transfer (EPT) and/or proton followed by electron transfer. It gives rise to radical ·O-Bp-NO_2 and is responsible for the low yield of O-Bp-NO_2H.

TABLE III Fitted parameters in the rate constant equation, r_{T_1}[a]$=k\times$[Q]$+b$ (Q: acid or HO-Bp-NO_2 respectively).

Quencher	k[b]/$(10^9(\mathrm{mol/L})^{-1}\mathrm{s}^{-1})$	b[c]/$(10^5\ \mathrm{s}^{-1})$
acid	8.3±0.9	0.7±1.5
HO-Bp-NO_2	5.6±0.2	1.1±0.1

[a] r_{T_1} is the measured pseudo-first order decay rate of ^{3}HO-Bp-NO_2;
[b] k is its second order reaction rate constants towards quenchers;
[c] b is the decay rate in neat acetonitrile without any proton donors. It may be resulted from triplet-triplet annihilation *etc.*

Supplementary materials: FIG. S1−S8 provide molecular structure and spin density contribution of O-Bp-NO_2H, kinetic curve at 450 nm of HO-Bp-NO_2 in acetonitrile solution containing various concentration of acid and kinetics at 650, 450, and 380 nm in neat acetonitrile solution with different concentrations of HO-Bp-NO_2 *etc.*

V. ACKNOWLEDGMENTS

This work was supported by the National Natural Science Foundation of China (No.21973082).

[1] D. R. Weinberg, C. J. Gagliardi, J. F. Hull, C. F. Murphy, C. A. Kent, B. C. Westlake, A. Paul, D. H. Ess, D. G. McCafferty, and T. J. Meyer, Chem. Rev. **112**, 4016 (2012).
[2] T. T. Eisenhart and J. L. Dempsey, J. Am. Chem. Soc. **136**, 12221 (2014).
[3] M. D. Sevilla and A. Kumar, Chem. Rev. **110**, 7002 (2010).
[4] H. Wang, X. Chen, and W. Fang, Phys. Chem. Chem. Phys. **16**, 25432 (2014).

[5] M. H. Stockett, Phys. Chem. Chem. Phys. **19**, 25829 (2017).
[6] C. T. Middleton, K. de La Harpe, C. Su, Y. K. Law, C. E. Crespo-Hernandez, and B. Kohler, Annu. Rev. Phys. Chem. **60**, 217 (2009).
[7] C. J. Gagliardi, B. C. Westlake, C. A. Kent, J. J. Paul, J. M. Papanikolas, and T. J. Meyer, Coord. Chem. Rev. **254**, 2459 (2010).
[8] S. J. Mora, E. Odella, G. F. Moore, D. Gust, T. A. Moore, and A. L. Moore, Acc. Chem. Res. **51**, 445 (2018).
[9] J. L. Dempsey, B. S. Brunschwig, J. R. Winkler, and H. B. Gray, Acc. Chem. Res. **42**, 1995 (2009).
[10] N. Hoffmann, Eur. J. Org. Chem. **2017**, 1982 (2017).
[11] D. Gust, T. A. Moore, and A. L. Moore, Acc. Chem. Res. **42**, 1890 (2009).
[12] J. C. Lennox, D. A. Kurtz, T. Huang, and J. L. Dempsey, ACS Energy Lett. **2**, 1246 (2017).
[13] P. Goyal and S. Hammes-Schiffer, ACS Energy Lett. **2**, 512 (2017).
[14] B. C. Westlake, M. K. Brennaman, J. J. Concepcion, J. J. Paul, S. E. Bettis, S. D. Hampton, S. A. Miller, N. V. Lebedeva, M. D. E. Forbes, A. M. Moran, T. J. Meyer, and J. M. Papanikolas, Proc. Natl. Acad. Sci. USA **108**, 8554 (2011).
[15] P. Goyal and S. Hammes-Schiffer, J. Phys. Chem. Lett. **6**, 3515 (2015).
[16] C. Ko, B. H. Solis, A. V. Soudackov, and S. Hammes-Schiffer, J. Phys. Chem. B **117**, 316 (2013).
[17] P. Goyal, C. A. Schwerdtfeger, A. V. Soudackov, and S. Hammes-Schiffer, J. Phys. Chem. B **119**, 2758 (2015).
[18] E. F. Plaza-Medina, W. Rodriguez-Cordoba, and J. Peon, J. Phys. Chem. A **115**, 9782 (2011).
[19] M. M. Brister, L. E. Piñero-Santiago, M. Morel, R. Arce, and C. E. Crespo-Hernández, J. Phys. Chem. Lett. **7**, 5086 (2016).
[20] R. A. Vogt, C. Reichardt, and C. E. Crespo-Hernández, J. Phys. Chem. A **117**, 6580 (2013).
[21] R. A. Vogt and C. E. Crespo-Hernández, J. Phys. Chem. A **117**, 14100 (2013).
[22] M. M. Brister, L. E. Piñeo-Santiago, M. Morel, R. Arce, and C. E. Crespo-Hernández, J. Phys. Chem. A **121**, 8197 (2017).
[23] Z. I. García-Berríos and R. Arce, J. Phys. Chem. A **116**, 3652 (2012).
[24] R. Arce, E. Pino, F. C. Valle, I. Negrón-Encarnación, and M. Morel, J. Phys. Chem. A **115**, 152 (2011).
[25] R. Arce, E. Pino, F. C. Valle, and J. Ágreda, J. Phys. Chem. A **112**, 10294 (2008).
[26] Z. I. García-Berríos, R. Arce, M. Burgos-Martínez, and N. D. Burgos-Polanco, J. Photochem. Photobio. A **332**, 131 (2017).
[27] D. Zhang, P. Jin, M. Yang, Y. Du, X. Zheng, and J. Xue, J. Phys. Chem. A **122**, 1831 (2018).
[28] K. A. Zachariasse, Chem. Phys. Lett. **320**, 8 (2000).
[29] M. Hashimoto and H. O. Hamaguchi, J. Phys. Chem. **99**, 7875 (1995).
[30] R. Ghosh, A. Nandi, and D. K. Palit, Phys. Chem. Chem. Phys. **18**, 7661 (2016).
[31] P. Goyal, C. A. Schwerdtfeger, A. V. Soudackov, and S. Hammes-Schiffer, J. Phys. Chem. B **120**, 2407 (2016).
[32] P. Jin, J. Long, Y. Du, X. Zheng, and J. Xue, Spectrochim Acta A **217**, 44 (2019).
[33] M. E. Casida, C. Jamorski, K. C. Casida, and D. R. Salahub, J. Chem. Phys. **108**, 4439 (1998).
[34] R. E. Stratmann, G. E. Scuseria, and M. J. Frisch, J. Chem. Phys. **109**, 8218 (1998).
[35] R. Bauernschmitt and R. Ahlrichs, Chem. Phys. Lett. **256**, 454 (1996).
[36] A. D. Becke, J. Chem. Phys. **98**, 5648 (1993).
[37] C. Lee, W. Yang, and R. G. Parr, Phys. Rev. B **37**, 785 (1988).
[38] M. J. Frisch, G. W. Trucks, H. B. Schlegel, G. E. Scuseria, M. A. Robb, J. R. Cheeseman, G. Scalmani, V. Barone, B. Mennucci, G. A. Petersson, H. Nakatsuji, M. Caricato, X. Li, H. P. Hratchian, A. F. Izmaylov, J. Bloino, G. Zheng, J. L. Sonnenberg, M. Hada, M. Ehara, K. Toyota, R. Fukuda, J. Hasegawa, M. Ishida, T. Nakajima, Y. Honda, O. Kitao, H. Nakai, T. Vreven, J. A. Montgomery, Jr., J. E. Peralta, F. Ogliaro, M. Bearpark, J. J. Heyd, E. Brothers, K. N. Kudin, V. N. Staroverov, R. Kobayashi, J. Normand, K. Raghavachari, A. Rendell, J. C. Burant, S. S. Iyengar, J. Tomasi, M. Cossi, N. Rega, J. M. Millam, M. Klene, J. E. Knox, J. B. Cross, V. Bakken, C. Adamo, J. Jaramillo, R. Gomperts, R. E. Stratmann, O. Yazyev, A. J. Austin, R. Cammi, C. Pomelli, J. W. Ochterski, R. L. Martin, K. Morokuma, V. G. Zakrzewski, G. A. Voth, P. Salvador, J. J. Dannenberg, S. Dapprich, A. D. Daniels, Ö. Farkas, J. B. Foresman, J. V. Ortiz, J. Cioslowski, and D. J. Fox, *Gaussian 09, A.01*; Wallingford, CT: Gaussian, Inc., (2009).
[39] T. A. Oliver, Y. Zhang, A. Roy, M. N. Ashfold, and S. E. Bradforth, J. Phys. Chem. Lett. **6**, 4159 (2015).
[40] Z. R. Grabowski, K. Rotkiewicz, and W. Retting, Chem. Rev. **103**, 3899 (2003).
[41] P. Suppan, J. Mol. Spectr. **30**, 17 (1969).
[42] G. N. Vriens, Industrial and Engineering Chemistry **46**, 669(1954).
[43] N. J. Turro, *Modern Molecular Photochemistry*, Sausalito, CA: University Science Books, (1991).
[44] W. J. Leigh, E. C. Lathioor, and M. J. S. Pierre, J. Am. Chem. Soc. **118**, 12339 (1996).

DOI:10.1063/1674-0068/cjcp2006107